Synthesis and Properties of Main-Chain Liquid Crystalline Polyurethane Elastomers

XIANGDONG HE, XUDONG JIA, and XUEHAI YU*

Department of Chemistry, Nanjing University, Nanjing 210008, People's Republic of China

SYNOPSIS

Liquid crystalline polyurethane elastomers (LCPUE) have been synthesized by a two-step block copolymerization reaction. The main-chain LCPUEs are based on two biphenyl-type mesogenic diol chain extenders (HB_2 and HB_6), a poly(tetramethylene oxide) (PTMO) soft segment, and different diisocyanates, including 4,4'-diphenylmethane diisocyanate (MDI), toluene diisocyanate (TDI), hexamethylene diisocyanate (HDI), and 1,4-(3,5,5-trimethyl)cyclohexane diisocyanate (IPDI). The polyurethanes were characterized by FTIR dichroism, DSC, DMA, WAXD, and polarized optical microscopy. Most of the polyurethane samples exhibited nematic thermotropic liquid crystal behavior and had physical properties typical of thermoplastic elastomers. The liquid crystal properties are strongly related to the interaction between the hard and soft segments of the polyurethane. As the compatibility of the soft and hard segments increased, the thermal stability of the liquid crystal phase and the transition temperatures decreased and the range of the transition became narrower. Uniaxial extension analysis shows that two orientation mechanisms exist in the LCPUE systems. These samples had fairly high strength and modulus and good membrane-forming ability. © 1994 John Wiley & Sons, Inc.

INTRODUCTION

Liquid crystal (LC) polymers are macromolecular materials capable of forming ordered (anisotropic) liquids either in solution (lyotropic) or in the neat state upon heating (thermotropic). This arises from the presence of rigid, rodlike molecules (mesogens) either as part of the backbone or as side chains linked to a more flexible backbone. This anisotropic behavior imparts unique physical properties to the polymer in terms of its mechanical, optical, and electrical characteristics. Main-chain LC polymers can consist entirely of rigid rod units covalently joined together. They do not melt but form a lyotropic LC phase in solvents. Alternatively, they can consist of rigid units joined by flexible spacers that show thermotropic behavior on heating.[1] On the other hand, thermoplastic polyurethane elastomers are block copolymers of the $(A\text{–}B)_n$ type, consisting of alternating soft and hard segments. At service temperatures, the soft segment is in a viscous or rubbery state, whereas the hard segment is in a glassy or semicrystalline state. The soft segment provides elastic character to the polymer, whereas the hard segment provides dimensional stability by acting as thermally reversible and virtual cross-links and also as a reinforcing filler. The unusual properties of these copolymers are directly related to their two-phase structures. In conventional segmented linear polyurethanes, the soft segments are commonly of low molecular weight (600–3000) polyether or polyester macroglycols that are chain-extended with a low molecular weight diol to produce a hard-segment length with a distribution of molecular weight.

The driving force for phase separation in these systems is the incompatibility of the two segment types. A wide spectrum of physical properties and morphologies has been observed, depending upon

* To whom correspondence should be addressed.

Journal of Applied Polymer Science, Vol. 54, 207–218 (1994)
 CCC 0021-8995/94/020207-12

the composition and chemical structure of the hard and soft segments.[2-4]

The incorporation of low molecular weight mesogenic diol as a chain extender can produce an LC polyurethane block copolymer. Such a polyurethane may possess both the characteristics of an LC polymer combined with a thermoplastic elastomer character of the segmented polyurethane. These characteristics are expected to impart a wide service temperature range due to the semirigid, rod-containing hard segment as well as the anisotropic optical, electrical, magnetic, and mechanical properties of LC polymers. It is well known that even though LC elastomers with reactive groups for cross-linking have been described only a few publications have so far been concerned with LC thermoplastic elastomers.[5-7] In this investigation, a series of biphenyl-type mesogenic diol chain-extended polyetherurethanes were synthesized. The hard segments consisted of different diisocyanates and either 4,4′-bishydroxyethyloxybiphenyl (HB_2) or 4,4′-bishydroxyhexyloxybiphenyl (HB_6). The soft segment was based on poly(tetramethylene oxide) diol (PTMO) of molecular weight 1000. Several polymers of different segment content were prepared. The purpose of this work was to study the effect of the mesogenic chain extenders on the microphase morphology and physical and thermal anisotropic properties of these LC polyurethane elastomers (LCPUE).

EXPERIMENTAL

Materials

4,4′-Diphenylmethane diisocyanate (MDI) was purified by vacuum distillation (0.3 mmHg) until the boiling point was reached at 170°C. Hexamethylene diisocyanate (HDI), toluene diisocyanate (TDI) (unspecified isomers), and 1,4-(3,5,5-trimethyl)-cyclohexane diisocyanate (IPDI) were purchased from Aldrich Chemical Co. DMAc and DMF were dried over molecular sieves (5 Å). 1,6-Hexanediol and 1,2-diethanol were purchased from E. Merck and were used as received.

Synthesis

1-Bromohexanol

The reaction was carried out at reflux for 24 h by heating a mixture of 35.43 g 1,6-hexanediol and excess 40% hydrobromic acid, using benzene as the solvent. The organic phase was washed successively with NaOH, 10% HCl, H_2O, and saturated NaCl solution and then dried over anhydrous magnesium sulfate. The solvent was removed under vacuum to leave a residue that after distillation at reduced pressure (2.5 Torr/95°C) resulted in a yield of 67% (36.55 g).

Mesogenic Diol

The diol, 4,4′-bishydroxyhexyloxybiphenyl (HB_6), was prepared as follows: 10 g of 4,4′-dihydroxybiphenyl, 0.1 g of triethylbenzyl ammonium bromide, 5 g of potassium hydroxide, and 70 g potassium carbonate were stirred into 150 mL of DMF. The resulting slurry was heated to 100°C, and 6-bromohexanol was added dropwise. The reaction mixture was reacted for 24 h and poured into cold water. The precipitated solid was filtered and recrystallized twice, first from a 3 : 1 mixture of ethanol and DMF and then from 1-butanol, to give 9.4 g (30% yield) of HB_6, mp 172–174°C. This compound was previously synthesized with a reported melting point of 167–170°C.[8] ^{1}H-NMR and element analysis of HB_2 and HB_6 revealed the following data: ^{1}H-NMR (DMSO-d_6):

HB_2: δ = 3.7–4.0 ppm (— CH_2, 8H);
4.7–4.9 ppm (— OH, 2H);
6.9–7.1 ppm (Ar— H, 4H);
7.4–7.6 ppm (Ar— H, 4H).

HB_6: δ = 3.7–4.1 ppm (— CH_2, 12H);
4.7–4.9 ppm (— OH, 2H);
6.9–7.1 ppm (Ar— H, 4H);
7.4–7.6 ppm (Ar— H, 4H).

ANAL: Calcd for HB_2: C, 70.06%; H, 6.61%.
Found: C, 70.11%; H, 6.45%.
Calcd for HB_6: C, 74.58%; H, 8.87%.
Found: C, 74.49%; H, 8.59%.

Liquid Crystalline Polyurethanes

The LC polyurethanes were synthesized by the two-step condensation reaction (shown in Scheme 1). HDI, 1.37 g, and 2 drops of stannous octoate were dissolved in 15 mL of DMF in a heat-dried four-neck round-bottom flask fitted with a reflux condenser, mechanical stirrer, thermometer, and addition funnels charged with 10 mL of DMF and 2.54 g of PTMO (M_n = 981). Nitrogen was kept flowing

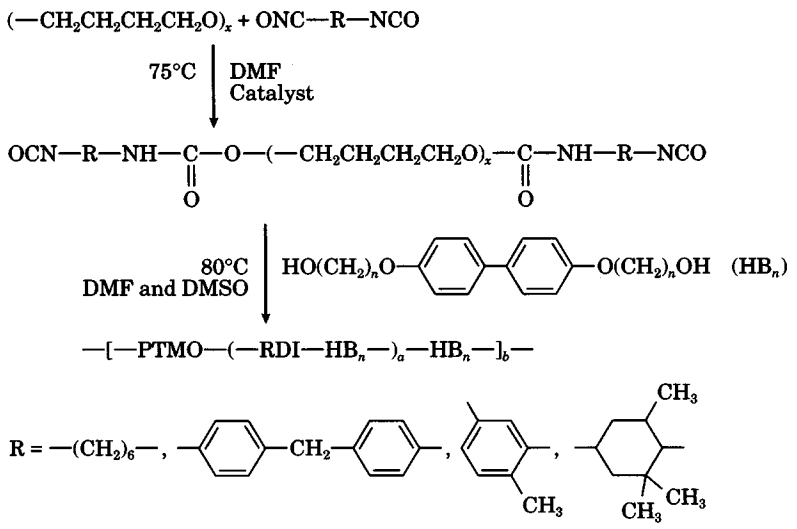

Scheme 1 Synthesis of Liquid Crystalline Polyurethane.

through the system. The PTMO solution was added dropwise below the flash point at 60°C, and the temperature was raised to 75°C. After 1.5 h, a solution of 2.0 g HB_6 in 20 mL DMSO was added dropwise to the above solution, and the temperature was raised to 80°C and kept there for 10 h. As the reaction proceeded, a mixed solvent system (DMF and DMSO) was added as needed to keep the solution clear throughout the reaction. By the end of the reaction period, the solution was poured into cold water to precipitate the polymer in the form of a white elastomeric material. The polymer was filtered, washed with fresh ethanol, and subsequently dried under vacuum at 60°C for 72 h.

Polymer Characterization

The intrinsic viscosities of the polymers were determined at 30°C in DMSO by using a Cannon-Ubbelohde viscometer.

Thermal analysis was carried out on a Perkin-Elmer DSC-2C interfaced with a Model 3600 data station using TADS software. Temperature and enthalpy calibration were carried out using indium and mercury as standards. A heating rate of 20 K/min under a 20 mL/min flow of dry air as the purge gas was used on samples of 10 ± 3 mg. The data processing unit allowed automatic subtraction of the base line and normalization of the thermogram for the sample weight.

Nuclear magnetic resonance experiments were carried out on a JEOL JNM-PMX COSI using tetramethylsilane (TMS) as an internal standard with the samples held at room temperature. All samples were prepared by dissolving about 5 mg of copolymer in 0.2–0.3 mL of deuterated chloroform. Wide-angle X-ray scattering patterns were obtained using monochromatic CuKα radiation (λ = 1.5418 Å) and a Nicolet Xentronics two-dimensional position-sensitive and data system. Data were collected for 20 min, and background scans of equivalent duration were subtracted to remove background scatter. The two-dimensional data were then azimuthally averaged to generate intensity vs. 2θ scans.

Dynamic mechanical data were obtained using a DDV-II-C apparatus that was controlled by a computer. All measurements were carried out under a nitrogen purge at a frequency of 110 Hz with a constant heating rate of 2 K/min.

Infrared survey spectra were recorded with a Nicolet 170SX Fourier transform infrared spectrophotometer operated with a dry-air purge. One hundred scans at a resolution of 2 cm^{-1} were signal-averaged before Fourier transformation. All IR spectra covered the range 400–4000 cm^{-1}. Uniaxial strain was applied by a stretching device, and IR measurements were carried out using Au polarizer inserted between the sample and the detector at 20°C.

Optical texture was studied with a Leitz-350 polarizing optical microscope equipped with a Linkam hot stage and a polaroid camera. The polymer sample was placed between glass slides and heated to the isotropic melt, and the slides were then sheared to produce a thin layer of melted polymer. The sample was then cooled at 10°C/min to room temperature and observed or photographed at that temperature.

RESULTS AND DISCUSSION

Polymer Synthesis

The polymers were prepared in a mixed-solvent system of DMF and DMSO. The solvent is crucial in determining whether a high molecular weight sample can be obtained by a two-step condensation reaction, because of the large differences in the solubility parameters of the soft and hard segments. It was found that a 5 : 4 ratio of DMF to DMSO could be used satisfactorily to prepare all the samples except those prepared using TDI. Relatively low molecular weight polyurethanes were obtained when the mixed TDI isomer was used as part of the hard segment. The reasons for these results are not clear, but similar observations have been reported in the literature.[9]

Infrared Spectroscopy

A typical IR spectra of PMB-6-69 is illustrated in Figure 1. The bands near 3330 (N—H stretch), 1700 (C=O stretch), 1540 (C—N—H bending), and 1280 cm^{-1} (N—C—O stretch) are attributed to the polyurethane hard segments.

Based on the NH band in the region of 3200–3500 cm^{-1}, the PMB-6-69 material appears to be primarily hydrogen-bonded, because the bonded NH peak at 3310 cm^{-1} predominates, whereas the free (nonhydrogen-bonded) NH peak at 3460 cm^{-1} is detectable only as a very small shoulder. In the carbonyl region between 1650 and 1750 cm^{-1}, the peak due to bonded C=O stretching centered at 1700 cm^{-1} predominates and that due to free C=O stretching appears as a shoulder at 1730 cm^{-1}. If it is assumed that the extinction coefficients of free and bonded C=O are approximately the same in polyurethanes,[10,11] the dominance of the bonded C=O peak indicates that a large fraction of the hard segments are hydrogen-bonded. This interurethane bonding is considered to occur in the interior of the hard domains. The intense H bonds form physical cross-links in the samples, which is one of the reasons that the samples exhibit thermally reversible rubber elasticity.

The IR spectra of other samples, which are not presented here, are very similar and indicate that nearly all the NH and C=O groups are hydrogen-bonded. It implies that the presence of LC brought about more aggregation of the hard segments, i.e., better microphase separation in LCPUE than those in more conventional segmented polyurethanes.

Optical Texture Analysis

Figure 2(a) and (b) show microphotographs of the LC chain extenders HB_6 and HB_2, which show nematic textures at temperatures of 140 and 180°C

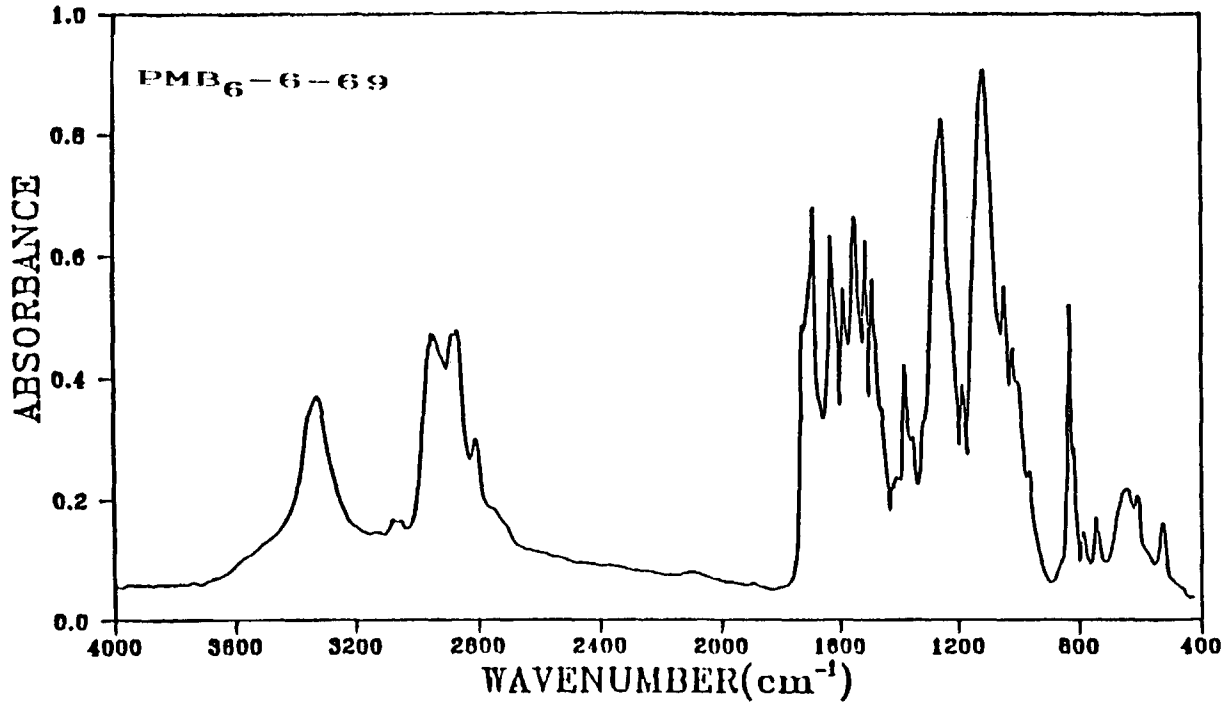

Figure 1 IR spectra of segmented polyurethane PMB_6-6-69.

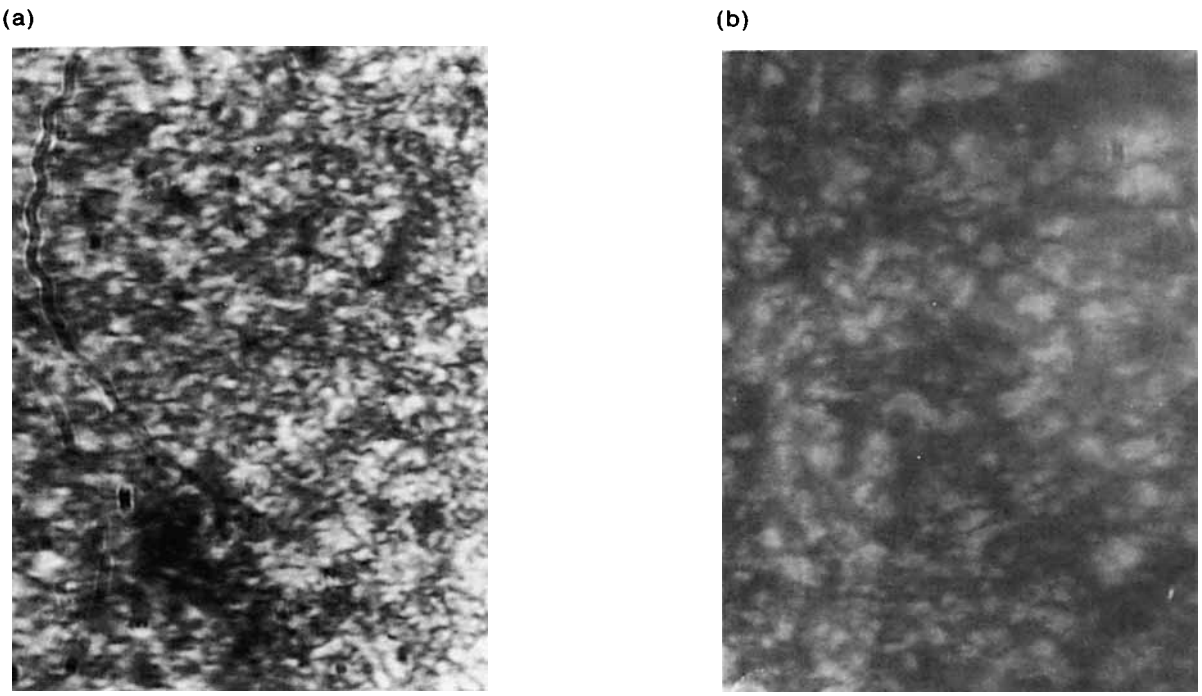

Figure 2 Textures of the nematic phase: (a) HB_6 at 140°C; (b) HB_2 at 180°C. Crossed polarizers.

respectively. It is noticeable that the increased of shear will result in the formation of a mesophase of a higher degree of order, i.e., a marble texture instead of a thread texture may be formed.

Figure 3 shows polarizing optical microphotographs of the polymer samples, in which the thread texture shown for PTB-9-65 is typical of a nematic LC polymer. Similar textures were observed in the other samples.

Thermal Analysis

DSC curves for the LCPUE are shown in Figure 4, and the thermal properties are summarized in Table I. All DSC data are for the first heating of the samples.

The DSC scans show that the LCPUE samples based on HDI and MDI have wider LC transition regions than those of polymers based on TDI. The melting-point order is $P_{MDI} > P_{HDI} > P_{IPDI} > P_{TDI}$. The LC phase transition region ($T_i - T_m$) or mesophase interval order is $P_{MDI} > P_{IPDI} > P_{HDI} > P_{TDI}$. This can be explained as due to the fact that hard segments of the TDI-based polyurethanes have a lower order than that of HDI- and MDI-based polyurethanes. The better compatibility between the hard and soft segments results in a decrease in the melting point. The higher melting point of the MDI series polymers is due to the better order of the rigid chain that approaches the decomposition temperature of the polyurethane. It can be observed that T_i and T_m decrease with increasing length of the spacer in the LC extenders by comparing the transition temperatures in PHB_6-9-56 and PHB_2-9-52. The complexity of multiendotherms in the MDI and HDI series around 100°C is due to the short-range ordering of the hard segments due to room-temperature annealing.

It can be seen from the data given in Table I that either an increase in the molecular weight or content of the soft segments results in a lower T_g, better microphase separation, and higher T_m and T_i.

Dynamic Mechanical Thermal Analysis

Rheovibron dynamic mechanical testing was used to study the dynamic moduli (E', E'') and internal friction (tan δ) as a function of temperature for −150 to 250°C. These typical samples PMB_6-9-61, PHB_6-9-56, and PTB_6-9-65 are illustrated in Figure 5. Two peaks designated γ and β appear in the tan δ data. The γ peak relaxation at −125°C, which is independent of sample composition, is a local mode motion of $-CH_2$ sequences in the polyether phase. The β peak corresponds to the glass transition of

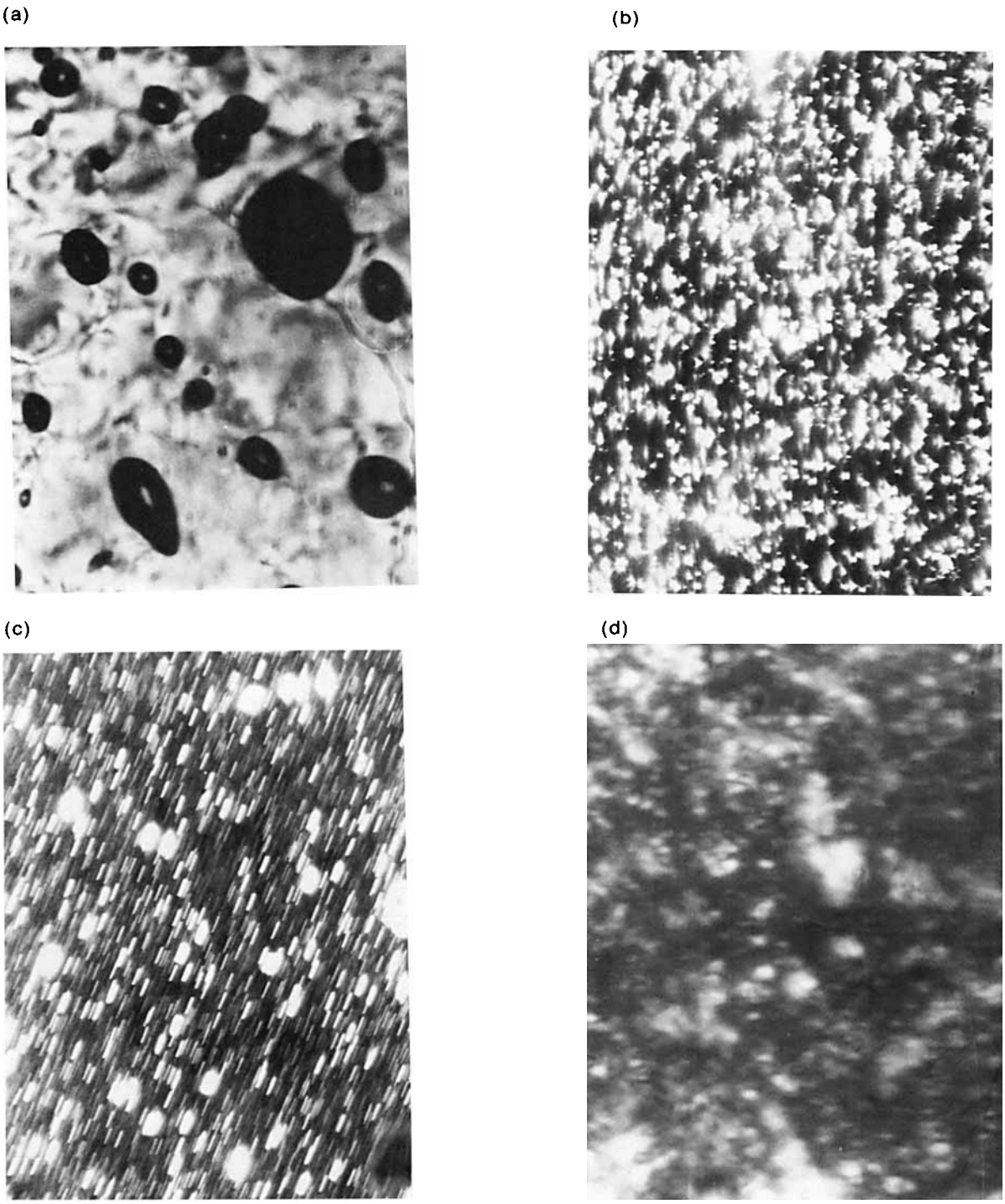

Figure 3 Textures of the nematic phase: (a) PTB_6-9-65, T = 100°C; (b) PIB_6-9-59, T = 145°C; (c) PHB_6-9-56, T = 145°C; (d) PMB_6-6-69, T = 250°C.

the polyether-rich soft-segment phase. E' decreases about two orders of magnitude in this transition region. Different isocyanates cause the β peak to move to higher temperatures and become broader in the order of MDI, HDI, and TDI. This indicates that compatibility between the hard and soft segments is in the order $PU_{MDI} < PU_{HDI} < PU_{TDI}$. The result is in agreement with the DSC data.

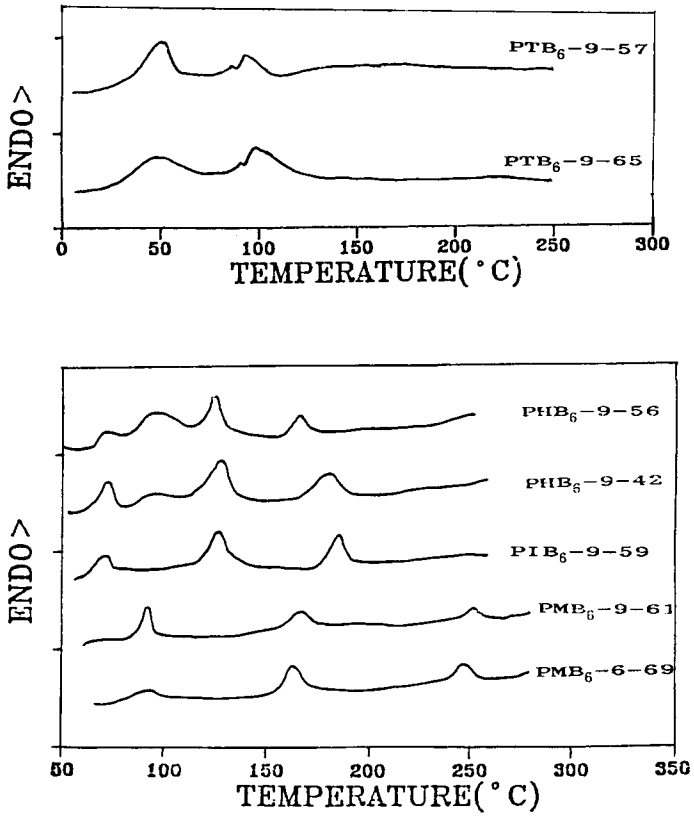

Figure 4 DSC traces of polyurethanes at heating of 20 K/min.

Interestingly, there are three loss peaks in the PMB_6-9-61 at high temperatures, which trend to the glass transition of the hard-segment phase and short-range order and long-range order in the hard-segment phase, respectively. It was rarely seen in the conventional polyurethanes. The PMB_6-9-61 shows an extended rubbery plateau modulus and a higher peak, which is defined as the hard-segment transition temperature. The MDI hard segment exhibited a more symmetric and rigid structure than did the HDI and TDI hard segments, which is indicative of a high-domain cohesion.

Table I Properties of LC Polyurethanes

No.	Sample Code	PTMO Molecular Weight	RDI	PTMO:RDI:HP_n	Yield (%)	$[\eta]$ (dL/g)	T_g (°C)	T_m (°C)	T_i (°C)
1	PHB_6-9-56[a]	981	HDI	1:3:2	93	0.81	−58.7	132	172
2	PHB_6-9-42	981	HDI	1:2:1	88	0.93	−64.3	127	183
3	PHB_6-6-65	685	HDI	1:3:2	75	0.47	−45.2	121	172
4	PIB_6-9-59	981	IPDI	1:3:2	70	0.31	−48.2	131	181
5	PTB_6-9-57	981	TDI	1:3:2	76	0.11	−47.5	86	95
6	PTB_6-9-65	981	TDI	1:4:3	70	0.11	−47.2	91	101
7	PMB_6-9-61	981	MDI	1:3:2	80	0.85	−52.2	167	252
8	PMB_6-6-69	685	MDI	1:3:2	79	0.80	−35.2	163	246
9	PHB_2-9-52	981	HDI	1:3:2	86	0.95	−47.7	140	210
10	PHB_2-9-38	981	HDI	1:2:1	87	0.59	−56.3	147	203
11	PHB_2-6-60	685	HDI	1:3:2	81	0.42	−33.1	141	200

[a] P refers to PTMO; H, to HDI; B_6, to HB_6 (B_2 to HB_2); 9, to 981 of PTMO molecular weight; and 56, to hard-segment content (%).

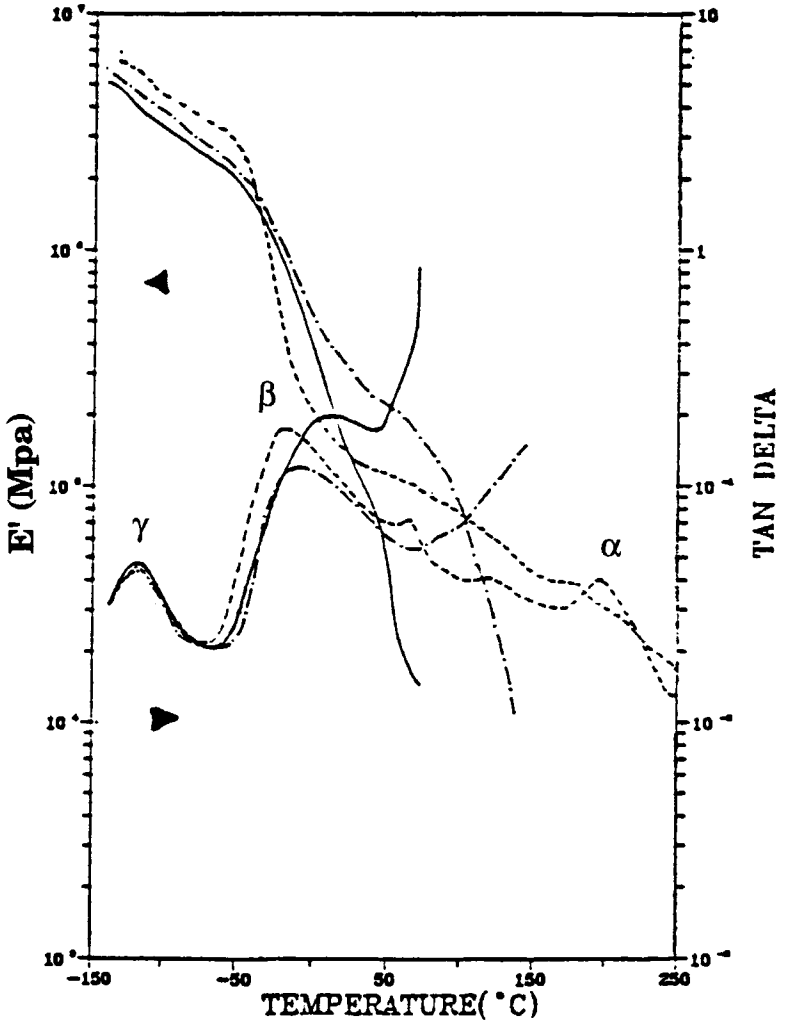

Figure 5 Dynamic mechanical spectrum of LCPUE: (——) PTB_6-9-65; (– · – ·) PHB_6-9-56; (- - - -) PMB_6-9-61.

Phase Behavior in WAXD Measurements

Figure 6 represents the WAXD patterns at different temperatures during heating from 20°C at 5°C/min for samples PHB-9-42 and PMB-9-61. At 20°C, PHB-9-42 and PMB-9-61 exhibit five and six sharp peaks, respectively, located between $2\theta = 10°$ and 25°. These peaks indicate that the samples possess relatively perfect crystalline regions. For PHB-9-42 and PMB-9-61, 103 and 110°C correspond to their melting points. Above 103 and 110°C, respectively, some peaks disappear ($2\theta = 19°$ and 21.6° for PHB-9-42; $2\theta = 22.9°$, 23.7°, and 24.7° for PMB-9-61), some peaks become weak ($2\theta = 20°$ and 23.2° for PHB-9-42 and $2\theta = 19.0°$ and 20.7° for PMB-9-61), and some new peaks appear ($2\theta = 22°$ for PHB-9-42 and 26° for PMB-9-61). The temperatures reveal the beginning of the crystal melting. Further heating to 123 and 252°C for samples PHB-9-42 and PMB-9-61, respectively, results in a diffuse equatorial reflection at 20°, a sharp and small peak at 3°, and a weak peak near 13°, which are characteristic of a nematic LC phase. Increasing temperature to 180°C for PHB-9-42 and 320°C for PMB-9-61 results in diffraction peaks in both samples that are quite diffuse with a maximum of about 20°, indicating a spacing of 4.5 Å, which is characteristic of an average distance between two neighboring chain molecules in the amorphous state. Similar results were obtained from a sample held in the melt for 10 h and then quenched into liquid nitrogen. A more detailed analysis of the diffraction data will be given elsewhere.

Orientation Analysis

Infrared dichroism can be used to study the orientation response of the hard and soft segments in

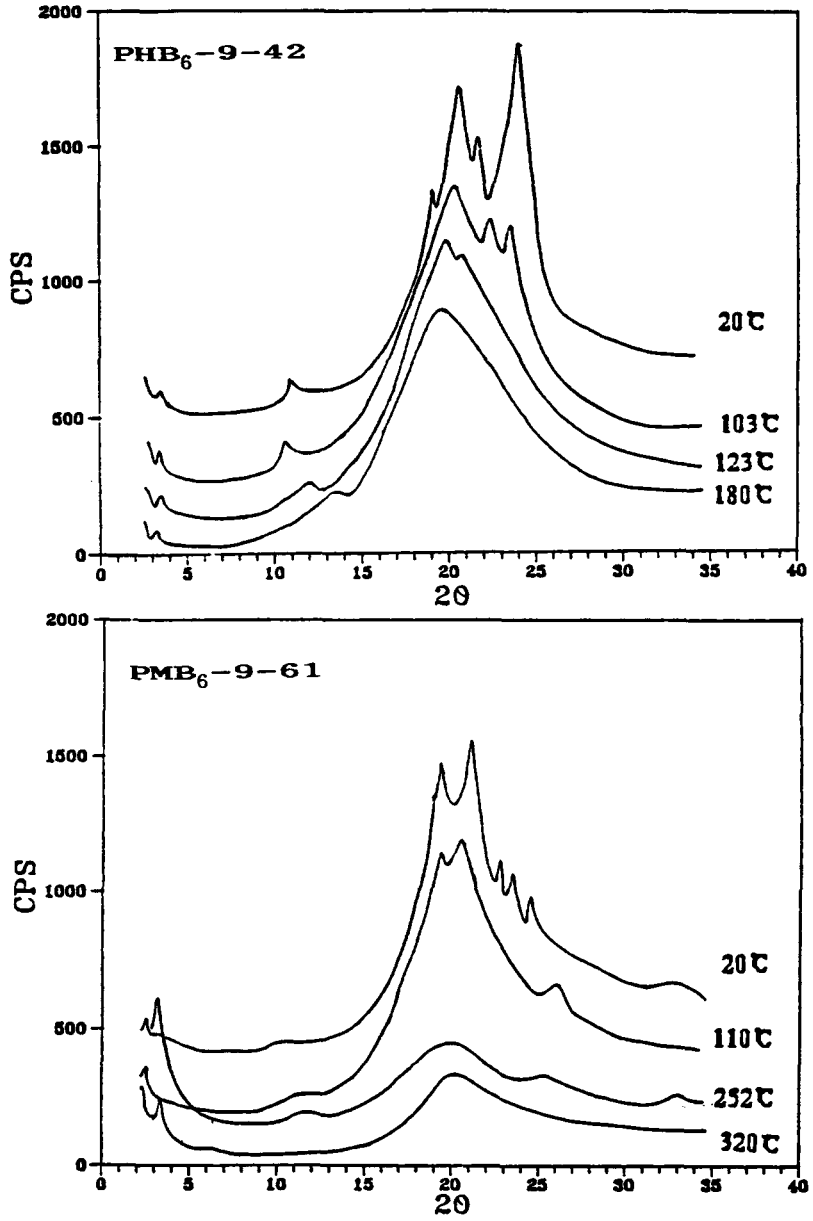

Figure 6 WAXD scanning of LCPUE under different temperatures: (a) PHB_6-9-42; (b) PHB_6-9-61.

polyurethane elastomers.[11-19] It will also be of prime importance for LCPUE since the rigid mesogen in the hard segment is expected to have a major effect on strain-induced orientation.

Orientation of the soft segment has been followed using the asymmetric CH_2 stretch vibration (2940 cm^{-1}). This group resides primarily in the soft segment. Hard block orientation was characterized by the NH group at 3310 cm^{-1}, which was located entirely in the hard segment, and the free carbonyl group vibration at 1730 cm^{-1} represents the orientation of the interface between soft and hard segments.[20]

The degree of orientational order in a polymer molecule can be defined by the degree of order F, which is measured relative to the long axis of the molecule:

$$F = \frac{3\langle \cos^2 \alpha \rangle - 1}{2} \quad (1)$$

where α is the angle between the individual molecular long axis and the brackets indicate the average value. The relation of an orientation function and infrared dichroism is

$$F = \frac{2x(D-1)}{(D+2)\langle 3\cos^2\alpha - 1\rangle} \quad (2)$$

The dichroic ration (D) may be calculated using the following equation:

$$D = \frac{A_\perp}{A_\parallel} \quad (3)$$

where $A_\perp$ and $A_\parallel$ are the absorbances measured with radiation polarized perpendicular and parallel to the stretching direction, respectively. When the vibrational transition moment is directed along axis of the molecule, we can write

$$F = \frac{D-1}{D+2} \qquad (\alpha = 0) \quad (4)$$

when the vibrational transition moment is perpendicular to long axis of the molecule, then

$$F = \frac{2-2D}{2+D} \qquad (\alpha = \pi/2) \quad (5)$$

The transition moment vectors of asymmetric vibration of CH_2, C=O, and NH stretching bands are reported to be oriented by about 90°, 78°, and 90°, respectively.[15-20] Thus, the orientation function described in eq. (5) will be followed. According to the above definition, a positive F implies that orientation is parallel to the stretch direction and a negative value of F relates to orientation transverse to the stretch direction.

Figure 7 shows the elongation dependence of the orientations of the CH_2, C=O, and NH functional groups, respectively. The orientation behavior of the CH_2 groups shows that the soft segment orients linearly with strain in the direction of the stretch. The orientation behavior of C=O and NH imparts information on the orientation of the hard-segment domains under uniaxial extension. In Figure 7, the hard-segment domains were found to initially orient transverse to the stretch direction. After reaching a maximum in negative orientation (elongation 200%), hard-domain crystallites appear to break up with increasing strain and orient positively. In contrast to —NH—, the F of free C=O reflects the orientation of groups at the interface between the hard and soft segments. The free C=O orients positively into the stretch direction, though as the elongation exceeds 200%, the slope of the curve turns negative.

The combination of the negative orientation of the hard segments and the positive orientation of the soft segment at low elongation has been previously observed,[15,17] and a few mechanisms to explain this orientation behavior have been proposed.[21,22] At relatively low elongations, the crystalline lamellae or glassy domains would be taken as orientation units floating in a matrix of the soft segments. In these units, the lamellar axis should be the principal orientation axis that provides for a positive orientation. Because the principal axis of urethane or urethaneurea linkage is perpendicular to the axis of lamellae or glassy domains, the initial lamellar orientation results in the negative orientation of hard segments. At relatively large elongation, on the other hand, the oriented lamellae disintegrates into small fragments. Then, the hard-segment axis turns out to be the principal orientation axis, resulting in a positive backbone orientation with further strain.

To support the IR dichroism observations of sample PMB-9-61, we studied its WAXD pattern as a function of strain (Fig. 8). With radiation po-

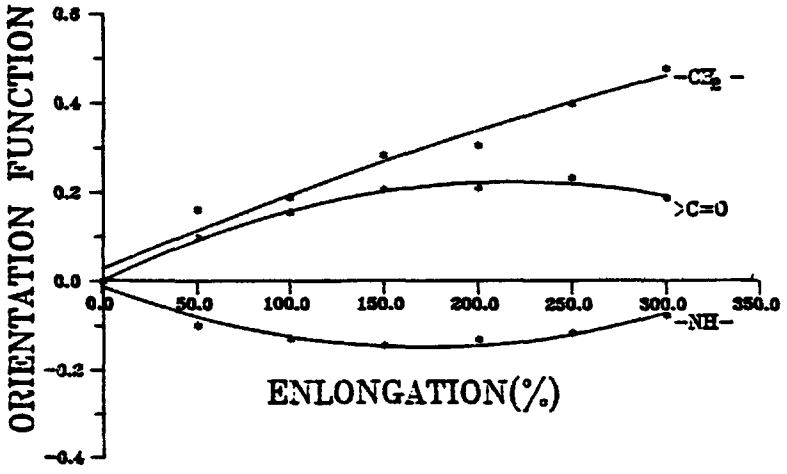

Figure 7 Orientation function F-elongation curves for PMB_6-9-61.

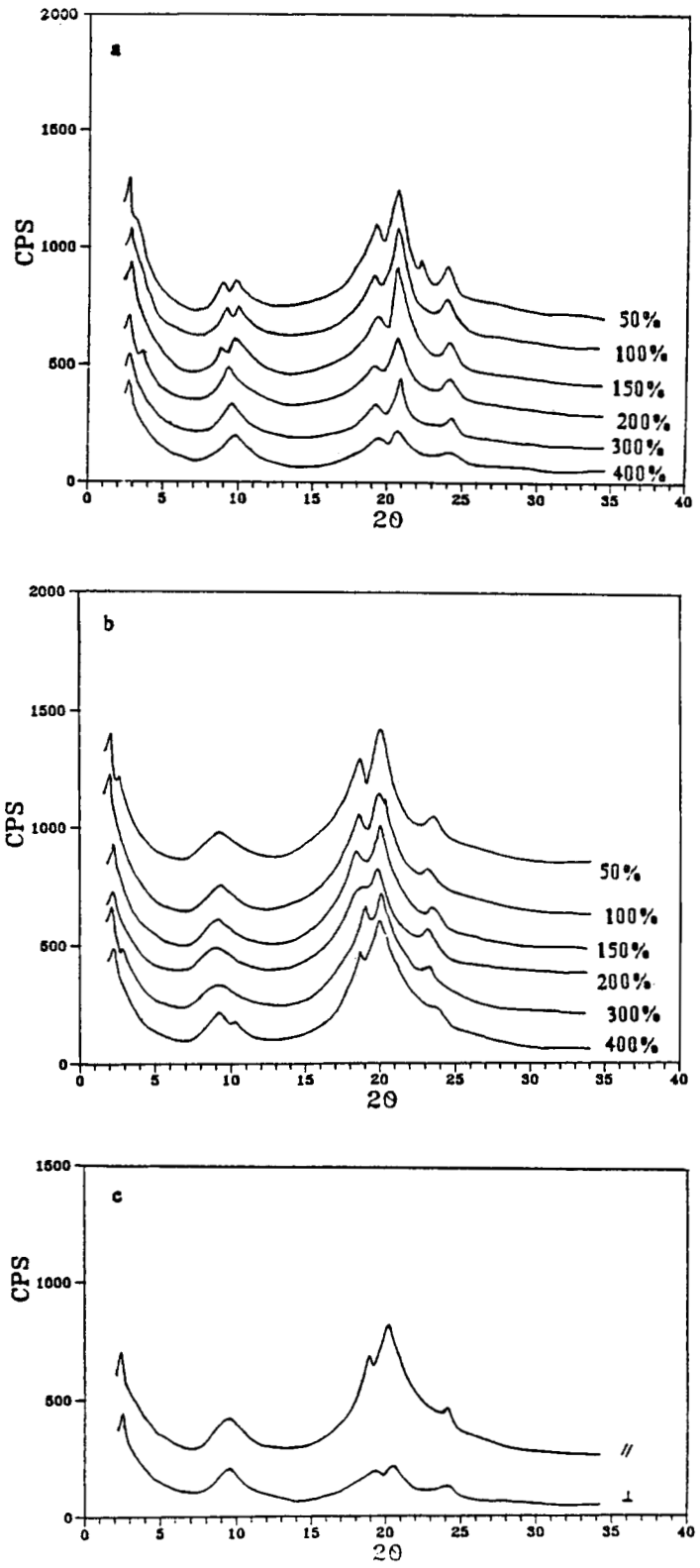

Figure 8 WAXD pattern of PMB_6-9-61 with various strains: (a) perpendicular to the stretching direction; (b) parallel to the stretching direction; (c) comparison of biaxial orientation with same strain.

larized parallel to the stretching direction, we can find greater crystalline-phase scattering intensity. With radiation polarized perpendicular to the stretching direction, the elongation is less than 200% and the crystalline peaks are essentially similar. As the elongation reaches 200%, the intensity of diffraction peaks at $2\theta = 21°$ start dropping rapidly, the value of d-spacing decreases, and the double peaks near 9° turn into a single peak. It is in consistent with IR dichroism.

CONCLUSION

It has been possible to synthesize block polyurethanes that are nematic LC polymers or both smectic and nematic in some samples. The formation of the LC phase is strongly related to the interaction of the soft and hard segments.

Greater compatibility between the hard and soft segments results in a decrease of the stability and the phase transition temperatures of the LC phase, and the mesophase interval becomes narrower. Most of the LCPUE are easily cast into films and have a fairly high modulus and strength.

The elongation of some samples reaches to 600%. Uniaxial extension by IR dichroism and WAXD analysis suggest that two orientation mechanisms exist in these LCPUE.

We acknowledge the National Science Foundation of the People's Republic of China for support of this work. We also express our appreciation to Dr. S. L. Cooper of Delaware University for his review of this manuscript.

REFERENCES

1. A. Ciferri, W. R. Krigbaum, and R. B. Meyer, *Polymer Liquid Crystals,* New York, Academic Press, 1982.
2. P. J. Flory, *Proc. R. Soc., Ser. A,* **234,** 73 (1956).
3. P. J. Flory and G. Ronca, *Mol. Cryst. Liq. Cryst.,* **54,** 289 (1979).
4. J. W. Hannell, *Polym. News,* **1**(1), 8 (1970).
5. K. Maejima and A. Niki, *Kobunshi,* **41,** 582 (1992).
6. W. Mormann and Baharifer, *Polym. Bull.,* **24,** 413 (1990).
7. W. Morman and B. Brahm, *Makromol. Chem. Rapid Commun.,* **9,** 175 (1988).
8. P. J. Stenhouse, W. Kantor, et al., *Macromolecules,* **22,** 1467 (1989).
9. M. Tanaka and T. Nakaya, *Kobunshi Ronbunshu,* **43,** 311 (1986).
10. C. S. P. Sung and N. S. Schneider, *Macromolecules,* **8,** 68 (1975).
11. C. B. Wang and S. L. Cooper, *Macromolecules,* **16,** 775 (1983).
12. S. Kohjiya, Y. Ikeda, S. Yamashita, M. Shibayama, T. Kotani, and S. Nomuya, *Polym. J.,* **23,** 991 (1991).
13. R. W. Seymour, G. M. Estes, and S. L. Cooper, *Macromolecules,* **3,** 579 (1970).
14. R. W. Seymour, A. E. Allegrezza, and S. L. Cooper, *Macromolecules,* **6,** 896 (1973).
15. G. M. Estes, R. W. Seymour, and S. L. Cooper, *Macromolecules,* **4,** 452 (1971).
16. J. C. West and S. L. Cooper, *J. Polym. Sci. Polym. Symp.,* **60,** 127 (1977).
17. H. Ishihara, I. Kimuya, K. Saito, and H. Ono, *J. Macromol. Sci. Phys.,* **B10,** 591 (1974).
18. Z. Wen, D. Shen, Q. Zhou, and X. Zhu, *Gao Fen Zi Xue Bao,* **2,** 206 (1991).
19. R. Zbinden, *Infrared Spectroscopy of High Polymers,* New York, Academic Press, 1964.
20. R. Bonart, L. Morbitzer, and E. H. Muller, *J. Macromol. Sci. Phys.,* **B9,** 447 (1974).
21. F. Hoffman and R. Bonart, *Macromol. Sci.,* **184,** 1529 (1983).
22. I. Kimura, H. Ishihara, H. Ono, N. Yoshihaya, S. Nomuya, and H. Kawai, *Macromolecules,* **7,** 355 (1974).

Received December 20, 1993
Accepted March 31, 1994